https://doi.org/10.46813/2021-134-024

AZIMUTHAL SURFACE WAVES IN LOW-DENSITY PLASMA LOADED, COAXIAL HELIX TRAVELING-WAVE-TUBE-LIKE WAVEGUIDES

I.O. Girka[1], M. Thumm[2]
[1]V.N. Karazin Kharkiv National University, Kharkiv, Ukraine;
[2]Karlsruhe Institute of Technology, IHM and IHE, Karlsruhe, Germany
E-mail: igorgirka@karazin.ua

The dispersion properties of flute electromagnetic waves propagating across an external axial static magnetic field in traveling-wave-tube-like waveguides with low-density plasma filling are investigated. The cylindrical structure consists of a central dielectric rod, placed inside a plasma coaxial layer with a metallic helix sheath on its outer interface, and a metal screen separated from the helix by another dielectric layer.

PACS: 52.40.Fd

INTRODUCTION

Traveling wave tubes (TWTs) are widely applied in telecommunication. That is why they are intensively studied in the leading scientific centers. A comprehensive overview of their development was presented in [1]. Their potential impact on commercial and industrial applications explains continuous interest in further improving their technical characteristics.

The dielectric-plasma-vacuum-metal structure considered in the present paper is almost the same as that studied in [2]. However, the following essential features are different. First, in [2] the azimuthal wavenumber m was equal to zero and wave propagation in axial direction was studied. On the contrary, flute electromagnetic waves with k_z=0 and $m\neq0$ are considered in the present paper. Second, in [2] the plasma was assumed to be degenerate, whereas a magnetoactive gas plasma is considered here.

Azimuthal surface waves (ASWs) are known to be eigen-electromagnetic waves of cylindrical plasma waveguides [3]. Therefore, they are studied in cylindrical coordinates (r is the radial coordinate, φ is the azimuthal angle), wherein the axis is directed along both the waveguide axis and the external static magnetic field. ASWs are intensively studied due to their possible applications in plasma electronics, plasma-antenna systems, plasma production and nano-technologies [4 - 11].

The spatial and temporal dependencies of ASW electromagnetic fields are as follows: $f(r)\exp[i(m\varphi-\omega t)]$ (the integer m is the azimuthal wavenumber, ω is the wave angular frequency, and t is the time). ASWs of ordinary polarization (OASWs) with the field components H_r, H_φ, E_z and those with extraordinary polarization (XASWs) with the components E_r, E_φ, H_z are known to propagate independently in the external axial static magnetic field.

In the present paper, the dispersion properties of coupled ASWs are studied in the case when the coupling is caused by the presence of a metallic helix, the slow-wave structure in TWTs. The following structure is considered: a cylindrical dielectric rod (for helix support) is placed inside a coaxial plasma layer with a cylindrical helix metallic sheath on its outer interface, and an additional dielectric coaxial layer, which is located between the helix and the outer cylindrical metal wall (Fig. 1). The latter dielectric layer is usually vacuum and is used in TWTs for transmission of an annular electron beam in axial direction.

The dispersion properties of ASWs in the same structure was studied in details in [12]. The case of a dense plasma, $\Omega_e>|\omega_e|$, was considered there in contrast to the present paper, where the case of a low-density plasma, $\Omega_e<|\omega_e|$, is studied. Here Ω_α is plasma frequency of the particle of species α ($\alpha = i$ for ions and $\alpha = e$ for electrons), and ω_α is the corresponding cyclotron frequency.

The paper is arranged as follows. After the present introduction the model of the plasma waveguide is described in Section 2. The spatial distribution of the ASW fields and the boundary conditions are presented, and the dispersion relation is derived there in the form of the determinant of an 8×8 matrix (the elements are listed in the Appendix). The dispersion relation is analyzed numerically in Section 3. Finally, the conclusions are summarized in Section 4.

1. PLASMA WAVEGUIDE MODEL AND DERIVATION OF DISPERSION RELATION

The three-component cylindrical waveguide structure (see Fig. 1) is assumed to be infinite and uniform in axial z-direction.

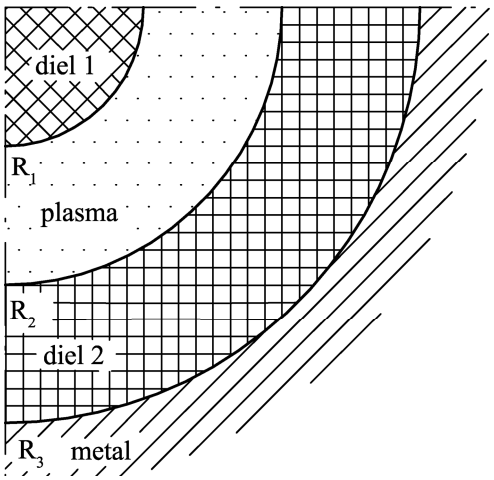

Fig. 1. Cross-section of the waveguide. The space $r\leq R_1$ is occupied by a dielectric rod. The plasma is placed in the layer $R_1\leq r\leq R_2$. The metallic helix sheath (similar to a tape helix) is placed at the interface $r=R_2$. The other dielectric layer, $R_2\leq r\leq R_3$, is located between the helix and the metal wall

The external static magnetic field is directed axially ($\vec{B}_0 \| \vec{z}$). A dielectric rod with dielectric constant ε_{d1} and radius R_1 is placed in the center of the metal waveguide with radius R_3. The radial distribution of the ASW axial magnetic field within the rod with account for the boundary condition at the axis of the system is written in terms of the Bessel function of the first kind of the order m [13], $J_m(\xi)$, as,

$$B_z(r) = A_1 J_m(k_{d1} r), r < R_1. \quad (1)$$

In (1), A_1 is a constant of integration, $k_{d1} = k\sqrt{\varepsilon_{d1}}$, $k = \omega / c$, and c is the speed of light in vacuum. The amplitudes of the radial and azimuthal components of the electric fields of ASWs can be derived in terms of $B_z(r)$ [3].

The radial distribution of the axial electric field reads as:

$$E_z(r) = A_2 J_m(k_{d1} r), r < R_1. \quad (2)$$

Then the amplitudes of the radial and azimuthal components of ASW magnetic fields can be written in terms of $E_z(r)$ [3], where A_2 is a constant.

The inner rod in covered by the coaxial plasma layer with internal radius R_1 and outer radius R_2. The tangential components of the electric and magnetic fields of ASWs should be continuous at the boundary $r = R_1$. The plasma is assumed to be cold and collisionless. In such a plasma, the electric displacement vector $\vec{D}$ is linked with the electric field $\vec{E}$ via the permittivity tensor [14].

The dispersion properties of XASWs in the case of strongly magnetized plasma, $\Omega_e > |\omega_e|$, were studied in [15]. In this case, surface type oscillations of ion species were demonstrated to be possible. Excitation of XASWs by annular ion beams was shown in [16] to take place under extremely strong external static axial magnetic field.

Within the plasma layer, the amplitude of the ASW axial magnetic field can be written in terms of the modified Bessel functions of the first, $I_m(\xi)$, and second, $K_m(\xi)$, kinds [13]:

$$B_z(r) = B_1 I_m(k_\perp r) + B_2 K_m(k_\perp r), R_1 < r < R_2. \quad (3)$$

Here B_1 and B_2 are the constants of integration. The penetration depth $k_\perp^{-1}$ of the XASW into the plasma is defined as follows: $k_\perp^2 = k^2 \varepsilon_1 (\mu^2 - 1)$, with $\mu = \varepsilon_2 / \varepsilon_1$. The electromagnetic wave field is of surface nature just inside the plasma coaxial layer. Outside of the plasma, the considered waves are of bulk nature. This is true within specific frequency ranges only. These ranges were presented in [15] from the inequality $k_\perp^2 > 0$:

$$\omega_{LH} < \omega < \omega_1 \quad \text{and} \quad \omega_{UH} < \omega < \omega_2, \quad (4)$$

where $\omega_{1,2} = \pm 0.5|\omega_e| + \sqrt{0.25\omega_e^2 + \omega_i |\omega_e| + \Omega_e^2}$ are the cut-off frequencies for bulk modes, and ω_{LH} and ω_{UH} are the lower and upper hybrid frequencies, respectively. The LF range, $\omega_{LH} < \omega < \omega_1$, is considered in the present paper.

The amplitudes of XASW electric fields can be written in terms of $B_z(r)$:

$$E_r(r) = \frac{k}{k_\perp^2}\left(\mu \frac{dB_z}{dr} + \frac{m}{r} B_z\right),$$

$$E_\varphi(r) = \frac{ik}{k_\perp^2}\left(\frac{dB_z}{dr} + \frac{\mu m}{r} B_z\right). \quad (5)$$

Within the plasma layer, OASWs are also of surface nature. The amplitude of their electric field reads as follows:

$$E_z(r) = B_3 I_m(k_o r) + B_4 K_m(k_o r), R_1 < r < R_2. \quad (6)$$

The penetration depth of OASWs into the plasma k_o^{-1} is defined as follows: $k_o = k\sqrt{-\varepsilon_3}$.

The outer interface of the plasma layer at $r=R_2$ is defined by the metallic helix sheath (tape helix). This sheath is assumed to be a surface with zero thickness and anisotropic electrical conductivity. The sheath is characterized by the helix pitch angle $\theta = arctan(d/(2\pi R_2))$ with d being the axial progression length of the tape helix, which is the angle between the tangent to the tape and the azimuthal direction. The electrical conductivity is assumed to be infinite along the tape and zero in the direction perpendicular to the tape. That is why at this interface, the tangential components of the ASW electric fields E_φ and E_z should be continuous, the longitudinal ASW electric field should vanish, which means $\sin\theta\, E_z + (+\cos\theta) E_\varphi = 0$, and the longitudinal ASW magnetic field should be continuous as well. These two last boundary conditions cause the coupling of XASWs and OASWs.

The coaxial plasma layer with the outer helix sheath is separated from the cylindrical metal wall by a coaxial dielectric layer with the dielectric constant ε_{d2}. The radial distribution of the ASW fields within this layer can be written in terms of Bessel functions of the first and second, $N_m(\xi)$, kinds [13]:

$$B_z(r) = C_1[J_m(k_{d2} r) N_m'(k_{d2} R_3) - N_m(k_{d2} r) J_m'(k_{d2} R_3), R_2 < r < R_3, \quad (7)$$

$$E_z(r) = C_2[J_m(k_{d2} r) N_m(k_{d2} R_3) - N_m(k_{d2} r) J_m(k_{d2} R_3), R_2 < r < R_3. \quad (8)$$

In (7) and (8), C_1 and C_2 are constants of integration, and $k_{d2} = k\sqrt{\varepsilon_{d2}}$. A prime denotes the derivative of the function with respect to the argument. The expressions (7) and (8) already satisfy the boundary conditions at the metal wall, which mean that the ASW tangential electric fields $E_\varphi(r)$ and $E_z(r)$ vanish at the interface $r=R_3$.

The boundary conditions mentioned above make it possible to derive the dispersion relation for ASWs in the considered waveguide in the form of the determinant of an 8×8 matrix:

$$deta_{ij} = 0. \quad (9)$$

The elements of the matrix a_{ij} are given in the Appendix.

2. NUMERICAL ANALYSIS OF THE DISPERSION RELATION

The effective azimuthal wavenumber, $k_{ef}=|m|\delta/R_1$, is chosen as abscissa ($\delta=c/\Omega_e$ is the skin-depth) in Figs. 2-7. Thus, these figures show the dependencies of the ASW eigenfrequencies on either the plasma particle density n_e (since $k_{ef}\propto n_e^{-1/2}$) or the dielectric rod radius R_1.

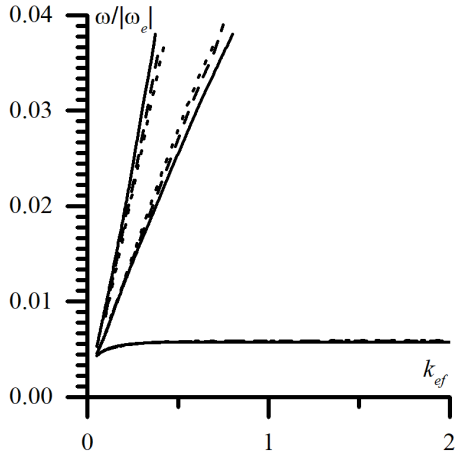

Fig. 2. ASW eigenfrequency vs k_{ef} for different $|m|$. $\theta=\pi/3$, $\varepsilon_{d1}=6.4$, $\varepsilon_{d2}=1$, $R_2=2R_1$, $R_3=3R_1$, $Z=0.2$. $m=+1$ (solid curves), $m=+2$ (dashed curves), $m=+3$ (dotted curves)

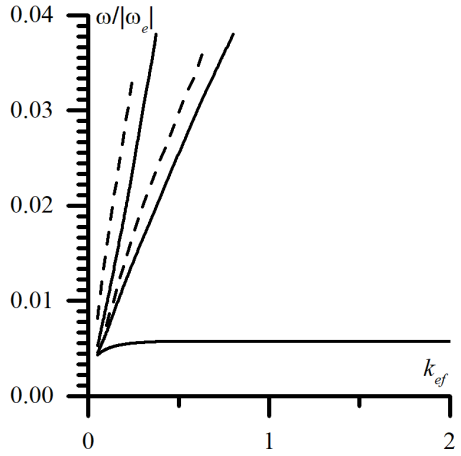

Fig. 3. ASW eigenfrequency vs k_{ef} for opposite directions of propagation. $\theta=\pi/3$, $\varepsilon_{d1}=6.4$, $\varepsilon_{d2}=1$, $R_2=2R_1$, $R_3=3R_1$, $Z=0.2$. $m=+1$ (solid curves), $m=-1$ (dashed curves)

The higher the radial wavenumber (the number of nodes of the radial field distribution within the dielectrics except of those at the axis and at the metal wall) is, the less efficient is the excitation of this wave (see, e.g. [17]). That is why the zeroth radial modes are considered in the present paper. To be sure that the calculated frequency relates to just the zeroth radial mode one has to check whether the frequency shift, $[k_{d1}R_1+k_{d2}(R_3-R_2)]$, is smaller than π.

To study the influence of the absolute value of the azimuthal wavenumber on the dispersion properties of ASWs the dependence of ASW eigenfrequencies on k_{ef} is plotted in Fig. 2 for the azimuthal wavenumbers $m=+1, +2, +3$. The dielectric constant of the inner rod is $\varepsilon_{d1}=6.4$ (mica), and the outer coaxial dielectric layer has $\varepsilon_{d2}=1$ (vacuum), since its purpose in a TWT is to carry the annular electron beam. The following other parameters of the waveguide structure are chosen for the calculations: $\theta=\pi/3$, $Z\equiv\Omega_e/|\omega_e|=0.2$, $R_2/R_1=2.0$, $R_3/R_1=3.0$. The difference between the three frequencies which corresponds to the given magnitude of the azimuthal wavenumber successively increases with increasing k_{ef}.

The difference between the ASW frequencies of the lower branch is almost invisible in Fig. 2. The lower frequency branch of the ASW with $m=2$ is larger than that for the ASW with $m=1$ by ≈2% for $k_{ef}=2.0$, and smaller than that for $m=3$ by ≈5%. The middle frequency branch monotonously increases with increasing $|m|$. The middle frequency branch of the ASW with $m=2$ is larger than that for the ASW with $m=1$ by ≈5% for $k_{ef}=0.4$, and smaller than that for $m=3$ by ≈5%. The upper frequency branch monotonously decreases with increasing $|m|$. The upper frequency branch of the ASW with $m=2$ is smaller than that for the ASW with $m=2$ by ≈11% for $k_{ef}=0.3$, and larger than that for $m=3$ by ≈ 4%.

To demonstrate the difference between the dispersion properties of ASWs propagating in opposite directions, the dependencies of their eigenfrequencies on the effective wavenumber are presented in Fig. 3 for the azimuthal wavenumbers $m=\pm1$. The other plasma waveguide parameters are the same as in Fig. 2. The main qualitative difference between the dispersion properties of ASWs with opposite signs of azimuthal wavenumbers is that the dispersion relation for ASWs with positive m have three roots rather than two as for the case of $m<0$. This peculiarity was noticed also for the case of dense plasmas [12]. These additional frequencies ($\omega<0.006\,|\,\omega_e|$ in Fig. 2) of ASWs with positive m are much lower than those in the middle and upper branches, which make them less important for excitation in TWTs. The frequencies of both upper and middle branches of ASWs with $m>0$ are smaller than those of ASWs with $m<0$. For example, for $k_{ef}=0.6$, the difference is ≈13%.

The influence of the helix pitch angle θ on the ASW eigenfrequency is shown in Fig. 4. In the case $\theta=\pi/2$ (see dashed curves), the infinite electrical conductivity of the metal helix sheath in axial direction suppresses the axial electric wave field, $E_z=0$. In this case ASWs propagate in the form of XASWs, and the dispersion relation has two roots. The dependence of the ASW eigenfrequency on k_{ef} for the helix pitch angle $\theta=\pi/3$ is presented in Fig. 4 by the solid curves, and for $\theta=\pi/6$ by the dotted curves. One can see a gradual decrease of the ASW frequency with increasing pitch angle of the helix sheath.

The influence of the geometrical dimensions of the waveguide components on the ASW eigenfrequency is studied in Fig. 5. The thin dash-dotted curves are presented for comparison of various different geometries with the case of equal widths of all the components of the waveguide structure under study: $R_2/R_1=2.0$, $R_3/R_1=3.0$. An increase of the dielectric rod radius R_1 by the factor 1.25, while keeping the same ratio of the two other radii, R_3/R_2, is shown by the dashed curves in Fig. 5 to cause an increase of the ASW eigenfrequencies.

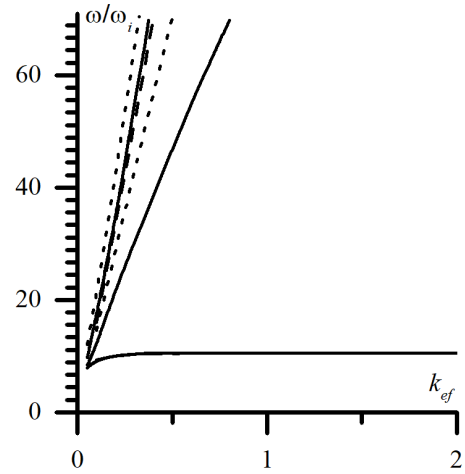

Fig. 4. ASW eigenfrequency vs k_{ef} for different pitch angles. ε_{d1}=6.4, ε_{d2}=1, R_2=2R_1, R_3=3R_1, Z=0.2. m=+1. θ=π/3 (solid curves); θ=π/2 (dashed curves); θ=π/6 (dotted curves)

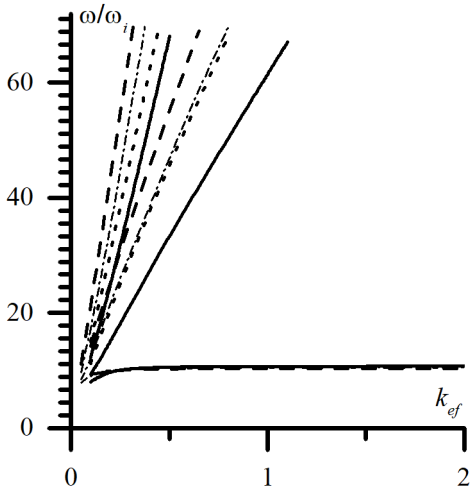

Fig. 5. ASW eigenfrequency vs k_{ef} for different dimensions of the elements. θ=π/3, ε_{d1}=6.4, ε_{d2}=1, m=+1, Z=0.2. R_2=2R_1, R_3=3R_1 (dash-dotted curves); R_2=3R_1, R_3=4R_1 (solid curves); R_2=1.6R_1, R_3=2.4R_1 (dashed curves); R_2=2R_1, R_3=4R_1 (dotted curves)

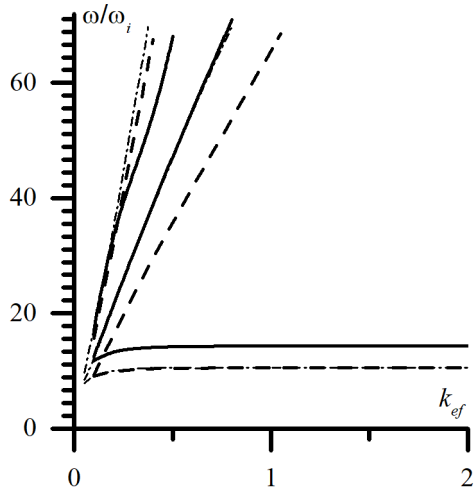

Fig. 6. ASW eigenfrequency vs k_{ef} for different dielectrics. θ=π/3, m=+1, Z=0.2. R_2=2R_1, R_3=3R_1. ε_{d1}=6.4, ε_{d2}=1 (dash-dotted curves), ε_{d1}=4.0, ε_{d2}=1 (solid curves), ε_{d1}=6.4, ε_{d2}=2 (dashed curves)

Increasing radius of the metal wall and the resulting increase of the width of the external dielectric layer, while keeping the same ratio of the two other radii, R_2/R_1=2.0, results in decreasing ASW frequencies (see dotted curves in Fig. 5). An increase of the width of the plasma layer, while keeping the same ratio of the external dielectric width to the radius of the dielectric rod, $(R_3-R_2)/R_1$, causes decreasing ASW frequencies (see solid curves). All the changes in the geometrical dimensions mentioned above only have a weak influence on the lower branch of ASW frequencies. The difference between the ASW frequencies in this branch is smaller than 4% for k_{ef}=2.

A decrease of the magnitude of the permittivity of the dielectric rod from ε_{d1}= 6.4 (dash-dotted curves) to ε_{d1}= 4.0 (solid curves) is shown in Fig. 6 to result in decreasing ASW eigenfrequencies of the upper branch, increasing eigenfrequencies of the lower branch with almost no change in the middle branch. Increasing magnitude of the dielectric constant of the outer dielectric layer from ε_{d2}=1.0 (dashed-dotted curves) to ε_{d2}=2.0 (dashed curves) causes decreasing ASW eigenfrequencies of the upper and middle branches with almost no change in the lower branch.

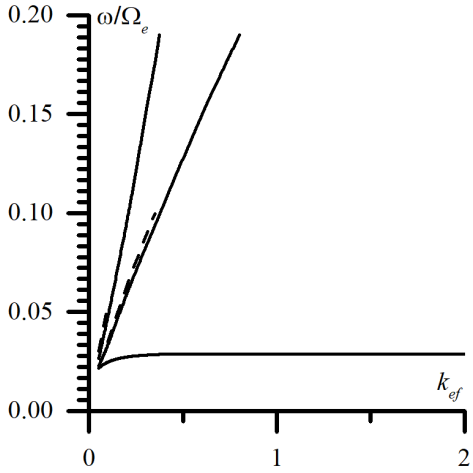

Fig. 7. ASW eigenfrequency vs k_{ef} for different magnitudes of the external static magnetic field. θ=π/3, ε_{d1}=6.4, ε_{d2}=1, m=+1, R_2=2R_1, R_3=3R_1. Z=0.2 (solid curves); Z=0.1 (dashed curves)

Fig. 7 shows that the increase of the external static axial magnetic field by the factor of two causes a weak increase of the ASW frequencies in the upper and middle branches and a shift of the ranges of the waveguide parameters, wherein ASWs propagate, to larger plasma particle densities and radii of the waveguide elements. No lower frequency was found for the case of Z=0.1.

In the following, the parameters of a practical laboratory device are estimated for which the results obtained in the present paper can be applied. If the external static axial magnetic field is B_0=1.5 kG, which is a typical magnitude for small-size TWTs, the angular electron cyclotron frequency is $|\omega_e|$=2.64·10^{10} rad/s. The highest frequency ω=0.038$|\omega_e|$ is obtained in calculations for k_{ef}=0.8, as shown in Figs. 2 and 3. Since $Z\equiv\Omega_e/|\omega_e|$=0.2, the electron plasma frequency is Ω_e=5.3·10^9 rad/s which corresponds to the plasma particle density n_e= 8.6·10^9 cm^{-3}. Applying this magnitude

for k_{ef} and taking the azimuthal wavenumber m =1 lead to the radius of the internal dielectric rod R_1=7.1 cm, the outer radius of the plasma coaxial layer R_2=14.2 cm, and that of the metal wall R_3=21.3 cm. These parameters look like achievable in a University Laboratory. The ASW frequency is expected to belong to the gigahertz range, ν = 0.16 GHz.

CONCLUSIONS

The dispersion properties of ASWs along with their excitation by annular beams of charged particles were studied in detail for the case of the cylindrical waveguide structure: central plasma column – coaxial dielectric layer – outer metal waveguide wall [3]. Two modes of ASWs: ordinary ASWs with the components E_z, B_r, B_φ, and ASWs with the components B_z, E_r, E_φ, were demonstrated to propagate independently in such structures.

Introduction of an internal dielectric rod (e.g. as helix support in a TWT) causes the appearance of an additional interface dielectric – plasma, which in turn gives rise to the existence of one more solution of the dispersion relation for the studied surface-type waves. This can be of practical interest for designing plasma electronic devices for wide-band communication systems.

Introduction of the cylindrical metallic helix sheath results in coupling of OASWs and XASWs. In this case, the zeroth radial modes of OASWs play the role of driven waves. The coupling causes the appearance of one solution more of the dispersion relation of ASWs with positive azimuthal wavenumbers. Since ASWs do not transfer their energy in axial direction, their excitation should be considered as an undesired parasitic phenomenon in such coaxial TWTs. Therefore, the analysis provided in the present paper can be useful to avoid parasitic energy losses. Decrease of the helix pitch angle is shown to result in an increase of the eigenfrequency of the undesired ASWs.

The waveguide structure under consideration is the same as studied in the previous paper [12]. The main difference of the present analysis from that carried out in [12] is that the plasma particle density of the coaxial plasma layer is assumed here to be small, $\omega_e^2>\Omega_e^2$, which is more typical for TWTs, rather than dense plasma particle density, $\omega_e^2<\Omega_e^2$, considered in [12].

Thus, the present detailed analysis of ASW dispersion properties in dependence on the waveguide parameters: geometrical dimensions, plasma particle density, external axial static magnetic field, magnitude and sign of azimuthal wavenumber, pitch angle of the metallic helix, and dielectric constants, can be of interest for suppression of parasitic waves in plasma loaded coaxial TWTs, operating in the GHz-range of frequencies.

APPENDIX

In (9), the matrix elements are as follows:

$$a_{11}=J_m\left(x_1\right),\ a_{13}=-I_m\left(x_3\right),\ a_{14}=-K_m\left(x_3\right),$$
$$a_{12}=a_{15}=a_{16}=a_{17}=a_{18}=0; \quad \text{(A1)}$$

$$a_{22}=J_m\left(x_1\right),\ a_{25}=-I_m\left(x_2\right),\ a_{26}=-K_m\left(x_2\right),$$
$$a_{21}=a_{23}=a_{24}=a_{27}=a_{28}=0; \quad \text{(A2)}$$

$$a_{32}=x_1J_m^{'}\left(x_1\right),\ a_{35}=-x_2I_m^{'}\left(x_2\right),$$
$$a_{36}=-x_2K_m^{'}\left(x_2\right),$$
$$a_{31}=a_{33}=a_{34}=a_{37}=a_{38}=0; \quad \text{(A3)}$$

$$a_{41}=x_1^{-1}J_m\left(x_1\right),\ a_{43}=x_3^{-1}I_m^{'}\left(x_3\right)+m\mu x_3^{-2}I_m\left(x_3\right),$$
$$a_{44}=x_3^{-1}K_m^{'}\left(x_3\right)+m\mu x_3^{-2}K_m\left(x_3\right),$$
$$a_{42}=a_{45}=a_{46}=a_{47}=a_{48}=0; \quad \text{(A4)}$$

$$a_{51}=a_{52}=a_{53}=a_{54}=a_{57}=0, a_{55}=I_m\left(x_4\right); \text{(A5)}$$

$$a_{56}=K_m\left(x_4\right),\ a_{58}=N_m\left(x_6\right)J_m\left(x_7\right)-J_m\left(x_6\right)N_m\left(x_7\right),$$
$$a_{63}=x_5^{-1}I_m^{'}\left(x_5\right)+m\mu x_5^{-2}I_m\left(x_5\right),$$
$$a_{64}=x_5^{-1}K_m^{'}\left(x_5\right)+m\mu x_5^{-2}K_m\left(x_5\right),$$
$$a_{67}=x_6^{-1}\left[J_m^{'}\left(x_6\right)N_m^{'}\left(x_7\right)-N_m^{'}\left(x_6\right)J_m^{'}\left(x_7\right)\right];$$
$$a_{61}=a_{62}=a_{65}=a_{66}=a_{68}=0; \quad \text{(A6)}$$

$$a_{71}=a_{72}=a_{73}=a_{74}=a_{75}=a_{76}=0,$$
$$a_{77}=x_8x_5^{-1}cos\theta\left[J_m^{'}\left(x_6\right)N_m^{'}\left(x_7\right)-N_m^{'}\left(x_6\right)J_m^{'}\left(x_7\right)\right],$$
$$a_{78}=sin\theta\left[J_m\left(x_6\right)N_m\left(x_7\right)-N_m\left(x_6\right)J_m\left(x_7\right)\right]; \text{(A7)}$$

$$a_{81}=a_{82}=0,\ a_{83}=sin\theta I_m\left(x_5\right),\ a_{84}=sin\theta K_m\left(x_5\right),$$
$$a_{85}=cos\theta x_4x_8^{-1}I_m^{'}\left(x_4\right),\ a_{86}=cos\theta x_4x_8^{-1}K_m^{'}\left(x_4\right),$$
$$a_{87}=sin\theta\left[N_m\left(x_6\right)J_m^{'}\left(x_7\right)-J_m\left(x_6\right)N_m^{'}\left(x_7\right)\right]; \text{(A8)}$$
$$a_{88}=x_6x_8^{-1}cos\theta\left[N_m^{'}\left(x_6\right)J_m\left(x_7\right)-J_m^{'}\left(x_6\right)NJ_m\left(x_7\right)\right].$$

The following notations are used in eqs. (A1)-(A8):

$$x_1=k_{d1}R_1,\quad x_2=k_oR_1,\quad x_3=k_\perp R_1,\quad x_4=k_oR_2,$$
$$x_5=k_\perp R_2,\ x_6=k_{d2}R_2,\ x_7=k_{d2}R_3,\ x_8=kR_2.$$

ACKNOWLEDGEMENTS

This work is partially supported by the Ministry of Education and Science of Ukraine Research Grant 0119U002526.

REFERENCES

1. D.F.G. Minenna, F. André, Y. Elskens, J.-F. Auboin, F. Doveil, J. Puech, É. Duverdier. The traveling-wave tube in the history of telecommunication // *The European Physical Journal H*. 2019, v. 44, p. 1-36.
2. M. Nejati, L. Rajaei. The effect of degenerate plasma on the frequency spectra of slow waves in helix traveling-wave tube // *IEEE Trans. Plasma Sci.* 2019, v. 47, № 5, p. 2571-2581.
3. V. Girka, I. Girka, M. Thumm. *Surface flute waves in plasmas. Theory and applications*. New York: "Springer-Verlag", 2014.
4. G.S. Nusinovich, Y. Carmel, A.G. Shkvarunets, J.C. Rodgers, T.M. Antonsen, V.L. Granatstein, Y.P. Bliokh, D.M. Goebel, J.P. Verboncoeur. The Pasotron: progress in the theory and experiments // *IEEE Transactions on Electron Devices*. 2005, v. 52, № 5, p. 845-856.
5. T. Anderson. *Plasma Antennas*. Boston, London: "Artech House", 2011.
6. I. Alexeff, T. Anderson, E. Farshi, N. Karnam, N.R. Pulasani. Recent results for plasma antennas // *Physics of Plasmas*. 2008, v. 15, № 5, p. 057104.

7. V.O. Girka, I.O. Girka, I.V. Pavlenko. Electrodynamic model of the gas discharge sustained by azimuthal surface waves // *Contributions to Plasma Physics*. 2001, v. 41, № 4, p. 393-406.
8. T. Ishijima, H. Toyoda, Y. Takanishi, H. Sugai. Design of large-area surface wave plasma excited by slotted waveguide antennas with novel power divider // *Japanese Journal of Applied Physics*. 2011, v. 50, № 3R, p. 036002.
9. K. Ostrikov, E.C. Neyts, M. Meyyappan. Plasma nanoscience: from nano-solids in plasmas to nano-plasmas in solids // *Advances in Physics*. 2013, v. 62, № 2, p. 113-224.
10. C.M. Ferreira, M. Moisan. *Microwave Discharges: Fundamentals and Applications*. "Springer Science and Business Media", 2013.
11. Yu.M. Aliev, H. Schlüter, A. Shivarova. *Guided-Wave-Produced Plasmas*. Berlin, Heidelberg: "Springer-Verlag", 2000.
12. I.O. Girka, I.V. Pavlenko, M. Thumm. Zeroth radial modes of azimuthal surface waves in dense plasma loaded, coaxial helix traveling-wave-tube-like waveguides // *Physics of Plasmas*. 2021, v. 28, № 4, p. 043106.
13. M. Abramowitz, I. Stegun. *Handbook of mathematical functions with formulas, graphs, and mathematical tables*. Washington: "National Bureau of Standards, Applied Mathematics Series", 1972.
14. A.F. Alexandrov, L.S. Bogdankevich, A.A. Rukhadze. *Principles of plasma electrodynamics*. Berlin: "Springer", 1984.
15. I.O. Girka, P.K. Kovtun. Azimuthal surface waves in a magnetized plasma // *Technical Physics*. 1998, v. 43, № 12, p. 1424-1427.
16. V.O. Girka, I.O. Girka, I.V. Pavlenko. Excitation of ion azimuthal surface modes in a magnetized plasma by annular flow of light ions // *Progress in Electromagnetics Research M (PIERM)*. 2011, v. 21, p. 267-278.
17. I.O. Girka, I.V. Pavlenko, M. Thumm. Excitation of higher radial modes of azimuthal surface waves in the electron cyclotron frequency range by rotating relativistic flow of electrons in cylindrical waveguides partially filled by plasmas // *Physics of Plasmas*. 2018, v. 25, № 5, p. 052109.

Article received 14.06.2021

АЗИМУТАЛЬНЫЕ ПОВЕРХНОСТНЫЕ ВОЛНЫ В ВОЛНОВОДАХ ТИПА ЛАМПЫ БЕГУЩЕЙ ВОЛНЫ С КОАКСИАЛЬНОЙ ВСТАВКОЙ ИЗ РАЗРЕЖЕННОЙ ПЛАЗМЫ

И.А. Гирка, М. Тумм

Исследованы дисперсионные свойства желобковых электромагнитных волн, распространяющихся поперек внешнего аксиального постоянного магнитного поля в волноводах типа лампы бегущей волны с коаксиальной вставкой из разреженной плазмы. Модельная цилиндрическая структура состоит из центрального диэлектрического стержня, окруженного коаксиальным плазменным слоем со спиралью на внешней поверхности и металлическим экраном, отделенным от спирали другим диэлектрическим слоем.

АЗИМУТАЛЬНІ ПОВЕРХНЕВІ ХВИЛІ У ХВИЛЕВОДАХ ТИПУ ЛАМПИ БІЖУЧОЇ ХВИЛІ З КОАКСІАЛЬНОЮ ВСТАВКОЮ З РОЗРІДЖЕНОЇ ПЛАЗМИ

І.О. Гірка, М. Тумм

Досліджено дисперсійні властивості жолобкових електромагнітних хвиль, які поширюються поперек зовнішнього аксіального сталого магнітного поля у хвилеводах типу лампи біжучої хвилі з коаксіальною вставкою з розрідженої плазми. Модельна циліндрична структура складається з центрального діелектричного стержня, оточеного коаксіальним плазмовим шаром зі спіраллю на зовнішній поверхні та металевим екраном, який відокремлено від спіралі іншим діелектричним шаром.